Iraqi Journal of Physics, 2019 *Vol.17, No.43, PP. 58-66*

DOI: 10.20723/ijp.17.43.58-66

Characterization of ZnO/GaAs heterojunction

Eman M. Nasir and Asmaa N. Mohammed Ali

Department of Physics, College of Sciences, University of Baghdad

E-mail: eman.itabi@gmail.com

Abstract

Thin films of ZnO are prepared by pulse laser deposition. These films were deposited on GaAs substrate to form heterojunction ZnO/GaAs solar cell. The effect of annealing temperatures at (RT, 373, 473) K on properties of structural and optical of ZnO thin films has been studied. The Diffraction analysis by X-ray indicated that all films have hexagonal polycrystalline structure. AFM shows that the grains uniformly distributed with homogeneous structure. The optical absorption spectra showed that all films have direct energy gap. The band gap energy of these films decreased with increasing annealing temperatures. From the electrical properties, the carriers have n-type conductivity. From C-V measurement of ZnO/GaAs heterojunciton at frequency 100, 200 kHz, It is found that built–in potential (V_{bi}) increases with increased frequency. As well as, from I-V characteristic it is observed that the ideality factor is 2.7. Short-circuit current (I_{sc}) is 4.0 mA/cm^2, open circuit voltage is 0.5 V, fill factor is 0.7 and the efficiency is about 6.0 %.

Key words

Thin films, optical properties, electrical properties, semiconducting, solar cell.

Article info.

Received: Aug. 2019
Accepted: Oct. 2019
Published: Dec. 2019

خصائص المفرق الهجين ZnO/GaAs

ايمان مزهر ناصر و اسماء ناطق محمد علي

قسم الفيزياء، كلية العلوم، جامعة بغداد

الخلاصة

حضرت اغشية رقيقة من ZnO بواسطة الترسيب بالليزر النبضي. رسبت هذه الأغشية على قواعد من GaAs لتحضير الخلايا الشمسية الهجينة ZnO / GaAs. درس تأثير درجات حرارة التلدين عند درجة حرارة (RT، 373، 473) K على الخواص التركيبية والبصرية لأغشية ZnO الرقيقة. بين تحليل الحيود بواسطة الأشعة السينية بأن جميع الأغشية لها بنية بلورية سداسية. يُظهر فحص AFM أن الحبيبات موزعة بشكل موحد مع بنية متجانسة. أظهرت أطياف الامتصاص البصري أن جميع الأغشية لها فجوة طاقة مباشرة، وتقل فجوة الطاقة لهذه الأغشية مع زيادة درجة حرارة التلدين. من دراسة الخواص الكهربائية، تمتلك الحاملات توصيلية من النوع n. و وجد من قياسات C-V للمفرق الهجين ZnO / GaAs وعند التردد 200 ,100، أن جهد البناء الداخلي (Vbi) يزداد بزيادة التردد. كذلك ،لوحظ من الخواص I-V، أن عامل المثالية هو (2.7) وتيار الدائرة القصيرة (Isc) هو 4.0 mA/cm^2، جهد الدائرة المفتوحة هو (0.5V) وعامل المليء هو (0.7) والكفاءة حوالي (0.7).

Introduction

Semiconductor thin films are important in industry due to their optical and electrical properties that used in many optoelectronic applications. zinc oxide have wide band gap (~3.3 eV) II-VI because showed several characteristics suited for several apparatus like transparent electrodes which work with the solar devices and antireflection coatings [1], it used in solar cell fabrication and steps of thermal treatment which required for improvement the photovoltaic properties. First step Range of temperature (350-5000) ^oC,

then deposition of the window substances [2]. It is necessary to detect effect of the post-thermal annealing on properties of the window thin films, wherever, it use as heterojunction materials in solar cells. Caban et al. have fabricated ZnO/GaAs heterojunction solar cells by the ALD method and found that ZnO films doped with Al effect on the photovoltaic properties of solar cell [3]. Makableh et al. have used ZnO as anti-reflection coating in GaAs solar cell; they observed a great enhancements in the properties of solar cell [4]. Eman et al. have studied the morphology and electrical properties of ZnO_x-CuO_{1-x} and found that roughness and conductivity increased with x content and decreased with annealing temperatures [5]. At present study, we studied effect temperature factor in annealing stage on material structural, electrical and optical properties of ZnO and fabricated of ZnO/GaAs heterojunction thin film solar.

Experimental

Pure zinc oxide (ZnO) were used as start materials to prepare films by pulsed laser deposition (PLD) technique on glass, GaAs substrates under vacuum of 3×10^{-3} mbar with 500nm of thickness, at different annealing temperatures using laser Nd:YAG at λ=1064 Nanometer, the pulse duration was 15 ns and the frequency was 6 Hz and at energy 800 mJ. The material was pressed into pellets (2 cm) in diameter and (0.25 cm) thickness, using hydraulic type (SPECAC), under pressure of 15 tons. finally the pellets were sintered in air at (500 K) for 2 h. 500 laser pulse is incident on the target surface by angle of 45°. 10 cm is the distance between the target and the laser, and 1.5 cm between the target and the substrate.

The composition structure of the thin films was determined by using (Philips X-ray diffractometer). Atomic force microscopy by AA3000 Angstrom advanced lmtd is used for studying morphology of surface of the prepared films, while the optical charterers is studied by spectrophotometer (Optima-3000). The electrical measurements include D.C conductivity; Hall Effect for ZnO films with different annealing temperatures has been studied.

The ability of the heterojunction was calculated by the reverse bias voltage at (0–1.2) V with two frequencies of (100 and 200) kHz by unit model (HP–R2C) 4275A and 4274A LRC meter. The current-voltage measurements in the dark were done using Keithly digital electrometer type 616 and D.C power supply and used light of halogen lamp at 25 mW/cm^2 (Philips Co).

Results and discussion

Determination of the structure of the ZnO films was done by using XRD to ensure the stoichiometry of our material. The Fig.1 shows XRD of thin films (ZnO) on glass substrates in many temperatures (as deposited, 373, 473) K for 1h, It can be noticed that they are three peaks for polycrystalline hexagonal ZnO phase located at 31.75◦, 34.4^o and 36.15^o with hkl (100), (002) and (110), respectively that is have dame with (JCPDS 96-900-4180) data as in Table 1. The crystallite size (grain diameter), D, of the ZnO films have been calculated by using the Scherrer's formula,

$$D = 0.9\,\lambda/\beta\cos\theta \qquad (1)$$

where:

λ is wavelength of X-ray, θ is half the angle between β and the scattered and incidents X-ray and β represent full width at half maximum. The values of grain size (G.S) decrease with increasing annealing temperatures and then decreased as given in Table1.

Similar result has been emphasized by Eman et al. [5] and Gupta et al. [6]. The increases in intensity and sharp peak in X-ray types showed the perfect crystallinity.

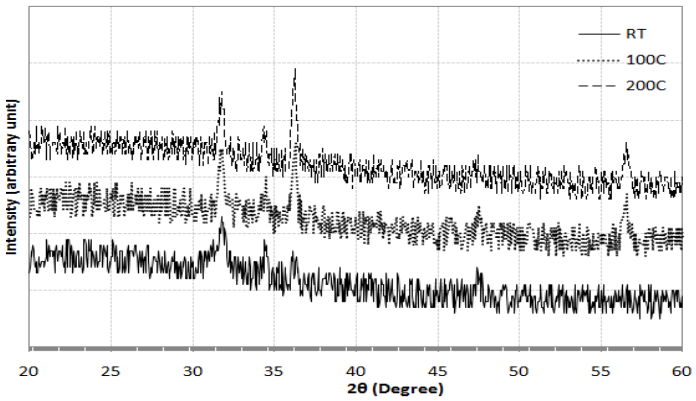

Fig.1: XRD patterns of ZnO thin films at different annealing temperatures (as deposited, 373, 473) K.

Table 1: XRD parameters of ZnO thin films at different annealing temperatures (as deposited, 373, 473) K.

Ta (K)	2θ (Deg.)	FWHM (Deg.)	d_{hkl} Exp.(Å)	G.S (nm)	d_{hkl} Std.(Å)	hkl
RT	31.75	0.2130	2.8160	38.8	2.8174	(100)
	34.4	0.2340	2.6049	35.5	2.6037	(002)
	36.15	0.3256	2.4827	25.7	2.4780	(101)
373	31.8	0.4103	2.8112	20.13	2.8174	(100)
	34.5	0.5275	2.5976	15.76	2.6037	(002)
	36.25	0.4689	2.4761	17.82	2.4780	(101)
	56.6	0.7034	1.6248	12.82	1.62661	(110)
473	31.65	0.4778	2.8196	17.28	2.8174	(100)
	34.5	0.2986	2.6095	27.83	2.6037	(002)
	36.25	0.2986	2.4801	27.98	2.4780	(101)
	56.65	0.4181	1.6274	21.56	1.62661	(110)

Parameters of AFM are included Peak-Peak, average roughness and diameter of size) of ZnO films deposited on glass substrates at RT and different temperatures have been determined using AFM analysis. Fig.2 shows 3D-AFM images for ZnO thin films at RT and many temperatures. It is observed from Table 2, that the average grain size values become more with elevating temperature and then decreased at 473 K and the ZnO film at 373 K have maximum values of Peak-Peak and roughness value. The results were a good agreement with El Sayed [7].

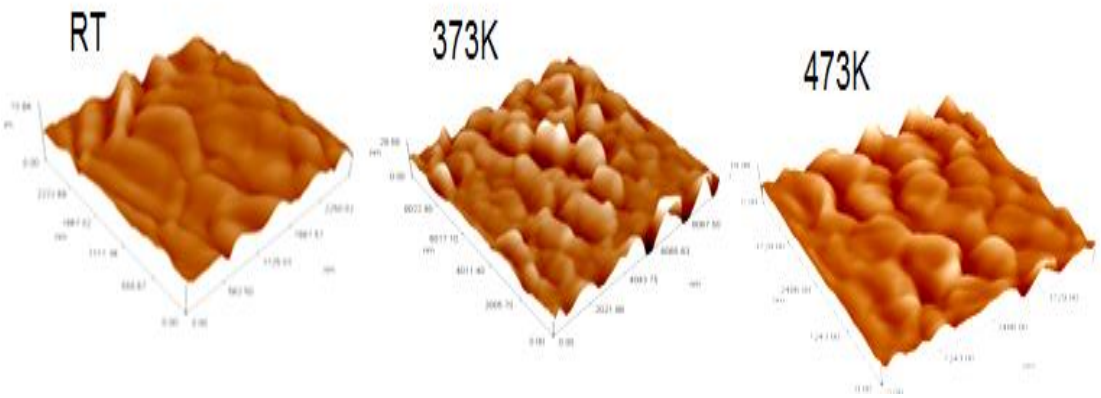

Fig. 2: 3D-AFM images for ZnO thin films at RT and different annealing temperatures.

Table 2: Average grain size, average roughness and Peak- Peak for ZnO thin films with different annealing temperatures (as deposited, 373 and 473) K.

Ta(K)	Ave. grain size (nm)	Ave. Roughness (nm)	Peak- Peak (nm)
RT	350.16	0.478	5.16
373	644.4	2.84	28.7
473	230.12	1.46	17.5

Fig.3 Transmittance spectrum of ZnO thin film on the glass at (200-1100) nm. It is observed from this figure that the values of transmittance decreases and shifting to higher wavelength with increasing annealing temperatures. The average optical transmittance is (75) %. As well as, results in to excellent optical quality that is agreed with the studies [8, 9].

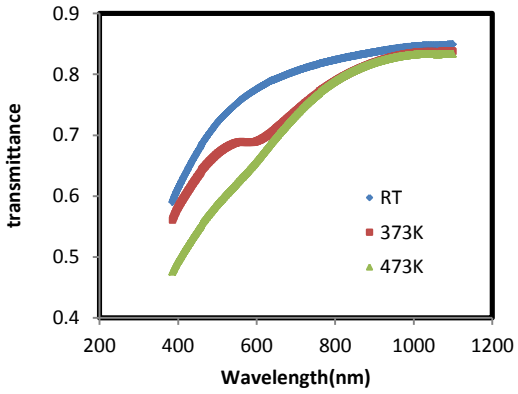

Fig.3: Transmittance spectrum of ZnO thin films at different annealing temperatures (as deposited, 373, 473) K.

Edge of the fundamental absorption in the semiconductors is depending on the exponential law [10].

$$\alpha h\nu = A\,(h\nu - Eg)^{r} \qquad (2)$$

A is constant factor

Eg is energy of optical band gap

r is any value between (1/2) and (3)

α is absorption coefficient and *h*νis photon energy

The absorption data is measured depended on Eq.(2) [10].

A is calculated based on equation [11]:

$$\alpha = \ln(1/T)/d \qquad (3)$$

d refer to film thickness.
$(\alpha h\upsilon)^2$ vs $h\upsilon$ refer to plot of the graph. By the optical methods, the direct band gap value of the produced ZnO films has been provided from $(\alpha h\upsilon)^2 = 0$. From Fig.4, *Eg* is decreased from 2.53-2.2 eV with increasing annealing temperatures from as depositing to 473K. The optical constant can be shown in Table 3 at wavelength 600 nm. It can be deduced that all optical constants become more with elevating temperatures [12].

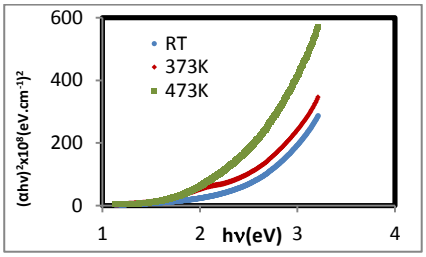

Fig.4: $(\alpha h\upsilon)^2$ as a function of hν for ZnO thin films at different annealing temperatures (as deposited, 373, 473) K.

Table 3: Optical properties parameters of ZnO films at different annealing temperatures.

T_a(K)	E_g(eV)	$10^4(\alpha^*cm)^{-1}$	n	K	ε_i	ε_r
RT	2.5	3.280	2.177	0.130	4.724	0.569
373	2.3	4.009	2.307	0.159	5.297	0.736
473	2.2	5.331	2.486	0.212	6.136	1.054

The change of electrical conductivity with temperature depending on the relation:

$$\sigma = \sigma_0 \exp(-E_a/ k_B T) \quad (4)$$

where E_a: is the thermal activation energy, T: is the absolute temperature, k_B: is the Boltzmann constant
σ_0: is the minimum electrical conductivity at 0 K.

Fig.5 demonstrates the plots of lnσ versus 10^3/T for ZnO films deposited at R.T and different annealing temperatures (100, 200) C in the range (273-473) K. From d.c measurements the conductivity ($\sigma_{d.c}$) become low with increasing of temperature in annealing stage and then increased, because the rearrangement is activated during the high temperature of annealing stage.

The activation energy conduction mechanism (E_{a2}) is activated at temperatures (443-473) K, but the activation energy (E_{a1}) is activated in lower temperatures (303-433) K. Influence of temperature on Ea_1 and Ea_2 for ZnO films is cleared as in Table 4. It is founded the energies activated increased with increasing of annealing temperatures.

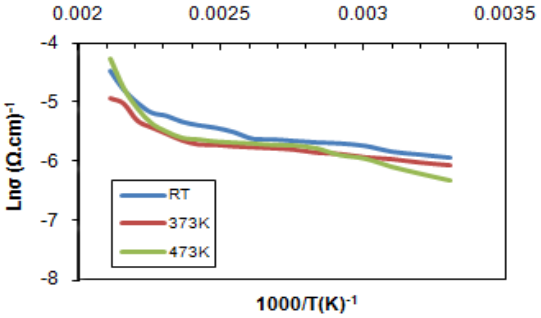

Fig.5: lnσ versus 10^3/T for ZnO films at different annealing temperatures.

Table 4: D. C. conductivity parameters for ZnO films at different annealing temperature.

T_a (K)	$\sigma_{d.cR.T}X10^{-5}$ $(\Omega.cm)^{-1}$	E_{a1} (eV)	Temp. Range (K)	E_{a2} (eV)	Temp. Range (K)
RT	2.61	0.056	303-433	0.42	443-473
373	1.69	0.061	303-383	0.59	393-473
473	1.78	0.064	303-443	0.60	443-473

The hall coefficient (R_H) is determined by measuring the Hall voltage that generates the Hall field across the sample of thickness (t), by:

$$R_H = \frac{V_H}{I}.\frac{t}{B} \quad (5)$$

Carriers concentration can be determined by using the relation

$$n_H = \frac{-1}{qR_H} \text{ for electrons,}$$

$$p_H = \frac{+1}{qR_H} \text{ for holes} \quad (6)$$

Hall's mobility (μ_H) can be written by

$$\mu_H = \frac{\sigma}{n.q} \quad (7)$$

$$\mu_H = \sigma |R_H| \quad (8)$$

the mobility of electron and hole, respectively,

$$\mu = \frac{V_d}{E} \quad (9)$$

where V_d is the drift velocity. So that we have

$$\sigma = (nq^2\tau)/m^* \quad (10)$$

where μ: is the mobility, τ: is the carrier's lifetime, *n*: is the carrier's concentration, m^*: is the effective mass of the carrier, and q: is the electron charge, Carriers concentration can be determined by using the relation

$$n_H = \frac{-1}{qR_H} \text{ for electrons,}$$

$$p_H = \frac{+1}{qR_H} \text{ for holes} \quad (11)$$

and mean free bath can be represented as

$L = V_d/\tau$

Hall mobility ($\mu_H = \sigma |R_H|$), drift velocity (v_d), carriers concentration (n_H), lifetime (τ) and mean free path (l) of charge carriers is calculated from Hall examinations. It can be noticed the whole films has negative Hall coefficient as shown in Table 5, the carrier's concentration reduce with elevating temperatures, but the Hall mobility become more when temperatures is increased. Also, the parameters lifetimeτ, drift velocity V_d and mean free path ℓ of the carriers have been determined as in Table 5. It is observed that all parameters approximately increase with increasing of annealing temperatures [11, 12].

Table 5: Hall parameters for ZnO films at different annealing temperatures.

T_s(K)	$\sigma_{R.T}\times10^{-5}$ $(\Omega.cm)^{-1}$	$n_H\times10^{14}$ (cm^{-3})	$\mu_H\times_{10}{}^{1}$ $(cm^2/V.sec)$	v_d (cm/s)	$\tau(s)\times10^{-9}$	$l\times10^{-9}$ (cm)
RT	3	2	18	0.93	1.30	1.20
373	0.22	0.13	60	1.58	1.47	2.33
473	0.02	0.01	83	0.03	1.65	2.93

Measurements (C-V) determines several factors parameters like junction capacitance (C), junction type and built-in potential (Vbi). The capacitance voltage of versus reverse bias was (0-1.2) volt with two frequencies 100 kHz and 200 kHz for ZnO /GaAs heterojunction as Fig.6. The capacitance reduces voltage of the reverse bias depending on equation:

$$C = dQ/dV \qquad (12)$$

The width of the junction can be deduced from the following equation:

$$W = \varepsilon_S / C_\circ \qquad (13)$$

where C_o is the capacitance at zero biasing voltage, and ($\varepsilon_s = \frac{\varepsilon_n \varepsilon_p}{\varepsilon_n + \varepsilon_p}$)

The concentration of carriers was calculated from the relation [11]:

$$\frac{1}{C^2} = \left[\frac{2(\varepsilon_p N_p + \varepsilon_n N_n)}{qN_p N_n \varepsilon_p \varepsilon_n}\right].(V_D - V) \qquad (14)$$

where $\left[2(\varepsilon_p N_p + \varepsilon_n N_n)/qN_p N_n \varepsilon_p \varepsilon_n\right]$ represent the slope. Fig. 7 is showing contrast C^{-2} with voltage. These data reveal the linear dependence in the reverse bias direction. The voltage axis provided the built-in potential value. It is observed that junctions have abrupt type (linear relation). The behavior is belonging to increasing width of depletion region (W) that results in increase in built– in voltage value and the V_{bI} value as Table 6. The effect of frequency was showed in Fig.6. It is noticed that the capacitance is reduce with elevating of frequency. Capacitance of the depletion layer indicates for charging increment on unit area depend on the changing with applied voltage. This means that behavior of the charge carriers transition was found as abrupt, that is determine by the relation between reverse bias and $1/C^2$ as a straight line. This result is in agreement reported by [13].

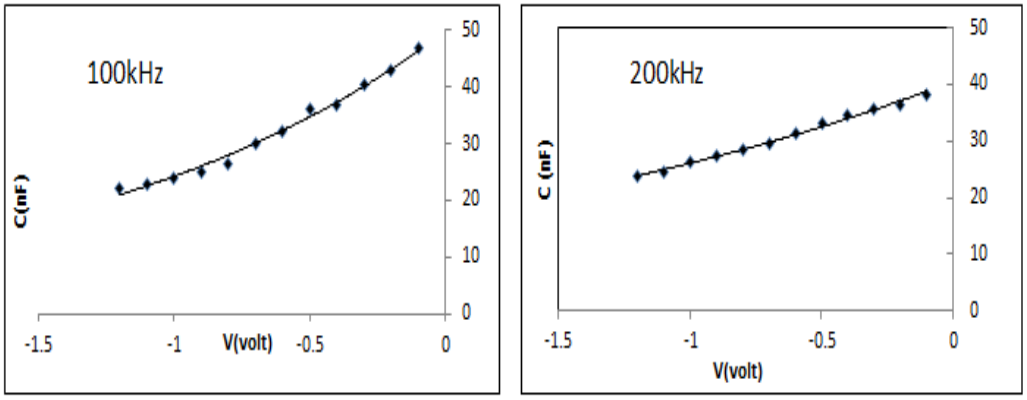

Fig.6: The variation of capacitance as a function of reverse bias voltage for ZnO/GaAs heterojunction at frequencies100 kHz and 200 kHz.

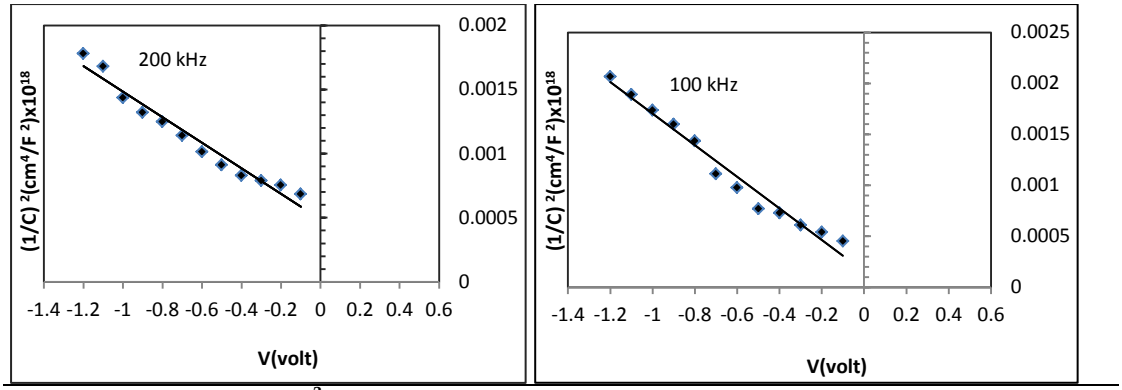

Fig.7: Variation of $(1/C)^2$ with voltage for ZnO /GaAs at frequencies100 kHz and 200 kHz.

Table 6: C-V parameters for ZnO /GaAs heterojunction at f=100 kHz and 200 kHz.

Frequency (kHz)	$C_o x10^{-9}$ (F/cm^2)	W (μm)	$nx10^{14}$ (cm^{-3})	V_{bi} (volt)
100	48	0.10	2.5	0.1
200	39	0.12	2.1	0.15

Using p-type GaAs substrate, ZnO/ GaAs heterojunction device was prepared, the results of the current-voltage (I-V) measurements of the ZnO /GaAs hetrojunctions were estimate under light and under dark conditions respectively as demonstrated in Fig.8. This figure shows that the variation of the current at dark condition is approximately a typical of ohmic conduction. Also it can be recognized two regions in this figure the first one represent the recombination current, while the second region represents the tunneling current. The first region could be approximated by an expression:

$I= I_o \exp(q V/\beta k_B T)$, where β is the ideality factor So the ideality factor has been calculated as in Table 7 and its about 2.7 which indicate that the junction have recombination tunneling mechanism.

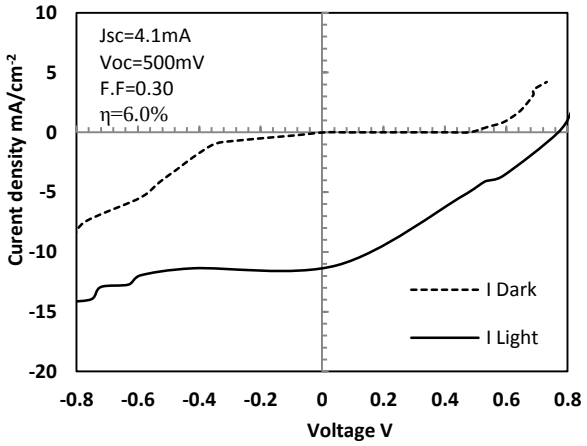

Fig. 8: I-V characteristics under dark and illumination for ZnO /GaAs.

Fig.8 demonstrates voltage of the open circuit (V_{oc}) and current of the short circuit (J_{sc}) were determined by intersects of photocurrent curve with x and y axis. Also maximum voltage (V_m) and current solar cell (I_m) were found. I_m and V_m are the current and voltage corresponding to the maximum power point. This is the point where maximum power can be

generated by the device. Full factor F.F and efficiency had been calculated as shown in Table 7. The fill factor given by the equation [11].

$$FF = V_m I_m / V_{oc} I_{sc} \text{ x } 100 \quad (15)$$

The efficiency(η) is another important parameter. It is a measure of the amount of light energy that is converted into electrical energy and is given by:

$$\eta = p_m / p_{in} = FF \times I_{sc} \times V_{oc} / p_{in} \times 100\% \quad (16)$$

where p_m is the area of the maximum power rectangle, and p_{in} is the incident power [11].

The photocurrent is important factor in the study, which plays an effective role in solar cells. Table 7 shows I-V parameters of ZnO /GaAs solar cell. This junction gave high value of efficiency (η= 6.0%). This result is in agreement with results by [13, 14].

Table 7: I-V parameters for ZnO /GaAs hetrojunctions.

T_a(K)	J_{sc} (mA/cm^2)	V_{oc} (V)	I_m (mA)	V_m(v)	F.F	η%	β
RT	4.10	0.5	4	0.4	0.7	6.0	2.9

Conclusions

All the prepared films by pulsed laser deposition technique exhibits n-type conductivity and have good structural and morphology and have two activation energies. The Electrical and photovoltaic characteristic of ZnO/GaAs heterojunction are strongly dependent on the illumination and frequency, while the C-V measurement reveled that both prepared device are abrupt. The photocurrent is important parameter that have effective role in manufacturing solar cells.

References

[1] R. R. Potter, Solar Cells, 16 (1986) 521-527.
[2] Y. S. Choi, C. G. Lee, S. M. Cho, Thin Solid Films, 289 (1996) 153-158.
[3] P.Caban, R.Pietruszka, K.Kopalko, B.S.Witkowski, K.Gwozdz, E.Placzek-Popko, M.Godlewski, Optik, 157 (2018) 743-749
[4] Y.F.Makableh, R.Vasan, J.C.Sarker, A.I.Nusir, S.Seal, M.O.Manasreh, Solar Energy Materials and Solar Cells, 123 (2014) 178-182.
[5] Eman Mizher Nasir, Asmaa N. Mohammed Ali, Kadhim A. Adem, Iraqi Journal of Physics, 14, 29 (2016) 8-14.
[6] B. Gupta, A. Jain, R. Mehra, J. Mater. Sci. Technol, 26, 3 (2010) 223-227.
[7] M. El Sayed, G. Said, S. Taha, A. Ibrahim, F. Yakuphanoglu, Super lattices and Microstructures, 62 (2013) 47-58.
[8] Ahmed M. Nawar, Nadia Abdel Aal, Nariman Said, Farid El-Tantawy, F. Yakuphanoglu, Journal of Applied Physics, 6, 4 (2008) 17-22.
[9] S. Thakur, N.Sharma, CODEN (USA), 5, 4 (2014) 18-24.
[10] J.I.Pankove,"Optical Process in Smei conductors" Dover Publications, New York, (1971).
[11] A.N. Donald, "Semiconductors Physics and Devices", University of New Mexico, IRWIN, Inc., (1992).
[12] Sarmad Fawzi Hamza, Journal of Babylon University, Pure and Applied Sciences, 21, 7 (2013) 2582-2588.
[13] J. Katayama Ito, M. Matsuoka, J. Tamaki, Journal of Applied Electro chemistry, 34, 7 (2004) 687-692.
[14] A. Tsukasaki, A. Ohtomo, T. Onuma, M. Ohtani, Nature Materials, 4 (2005) 42-46.